# Spatial targeting of type II protein kinase A to filopodia mediates the regulation of growth cone guidance by cAMP

Jianzhong Han, Liang Han, Priyanka Tiwari, Zhexing Wen, and James Q. Zheng

Department of Neuroscience and Cell Biology, Robert Wood Johnson Medical School, University of Medicine and Dentistry of New Jersey, Piscataway, NJ 08854

The second messenger cyclic adenosine monophosphate (cAMP) plays a pivotal role in axonal growth and guidance, but its downstream mechanisms remain elusive. In this study, we report that type II protein kinase A (PKA) is highly enriched in growth cone filopodia, and this spatial localization enables the coupling of cAMP signaling to its specific effectors to regulate guidance responses. Disrupting the localization of PKA to filopodia impairs cAMP-mediated growth cone attraction and prevents the switching of repulsive responses to attraction by elevated cAMP. Our data further show that PKA targets protein phosphatase-1 (PP1) through the phosphorylation of a regulatory protein inhibitor-1 (I-1) to promote growth cone attraction. Finally, we find that I-1 and PP1 mediate growth cone repulsion induced by myelin-associated glycoprotein. These findings demonstrate that the spatial localization of type II PKA to growth cone filopodia plays an important role in the regulation of growth cone motility and guidance by cAMP.

## Introduction

Guided axonal growth is essential for both the initial wiring of neuronal circuitry during development and the regeneration of synaptic connections in the adult nervous system after injury and diseases (Bahr and Bonhoeffer, 1994; Aubert et al., 1995; Tessier-Lavigne and Goodman, 1996; Harel and Strittmatter, 2006). The directional motility of the growth cone at axonal tips is regulated by a variety of environmental factors that either promote/attract or inhibit/repel the axonal elongation (Tessier-Lavigne and Goodman, 1996; Dickson, 2002). Although many families of guidance ligands and receptors have been recently identified (Tessier-Lavigne and Goodman, 1996; Dickson, 2002; Charron and Tessier-Lavigne, 2005), the intricate signaling cascades that control and regulate axonal growth and guidance remain to be fully understood. The second messenger, cAMP, represents an important intracellular signal that exhibits profound effects on growth cone motility and guidance. Previous studies have linked elevated cAMP signaling with enhanced elongation of growth cones (Richter-Landsberg and Jastorff, 1986; Rydel and Greene, 1988; Zheng et al., 1994b). The importance of cAMP regulation of axonal growth is further augmented by recent findings that manipulating the cAMP signaling pathway can overwrite the inhibitory/repulsive effects of some extracellular molecules on axonal growth, even converting them to attractive/positive responses (Song and Poo, 1999). For instance, an elevation of cAMP levels has been shown to convert myelin-associated glycoprotein (MAG)–induced growth cone repulsion to attraction in culture and promote axonal regeneration in vivo (Song et al., 1998; Qiu et al., 2002; Spencer and Filbin, 2004). Therefore, the cAMP pathway could be a potential target for therapeutic intervention to promote nerve regeneration after injury and degeneration (Filbin, 2003; Skaper, 2005).

At present, the exact signaling mechanisms underlying cAMP effects on growth cones remain unclear. The existence of the intricate cross talk of cAMP to other signaling pathways has added more complexity to this issue. For example, both $Ca^{2+}$ and cAMP are key second messengers involved in growth cone guidance by several extracellular cues, and $Ca^{2+}$-dependent turning responses can be modulated by the cAMP pathway: the elevation of cAMP levels dictates attraction, whereas the inhibition of PKA results in repulsion (Song and Poo, 1999). It has been proposed that cAMP signaling could affect the $Ca^{2+}$ signals elicited by extracellular cues through the modification of

Correspondence to James Q. Zheng: zhengjq@umdnj.edu

Abbreviations used in this paper: AKAP, a kinase-anchoring protein; BDNF, brain-derived neurotrophic factor; CaMKII, Ca-calmodulin–dependent kinase II; CaN, calcineurin; CM, control morpholino; DARPP-32, dopamine- and cAMP-regulated phosphoprotein of 32 kD; I-1, inhibitor-1; IM, I-1 morpholino; IP, immunoprecipitation; MAG, myelin-associated glycoprotein; NT-3, neurotrophin-3; OA, okadaic acid; PACAP, pituitary adenylate cyclase–activating polypeptide; PP1, protein phosphatase-1.

The online version of this article contains supplemental material.


The Journal of Cell Biology, Vol. 176, No. 1, January 1, 2007 101–111
http://www.jcb.org/cgi/doi/10.1083/jcb.200607128

Supplemental Material can be found at:
http://www.jcb.org/cgi/content/full/jcb.200607128/DC1

voltage-dependent $Ca^{2+}$ channels or $Ca^{2+}$ release from the intracellular $Ca^{2+}$ stores (Nishiyama et al., 2003; Henley et al., 2004; Ooashi et al., 2005). Our recent work suggests that PKA targets a downstream component in the $Ca^{2+}$ signaling pathway, protein phosphatase-1 (PP1), to allow the switching of repulsion to attraction (Wen et al., 2004). It is conceivable that cAMP could act at multiple steps in the $Ca^{2+}$ signaling pathway to affect growth cone behaviors, but how it specifically targets distinct downstream effectors remains to be investigated.

The cAMP molecule can diffuse over a long distance in the cytosol to activate a wide range of effectors (Kasai and Petersen, 1994), and its major effector, PKA, is a multifunctional enzyme with a broad substrate specificity (Shabb, 2001). Therefore, the mechanisms for spatiotemporal selectivity and efficiency in cAMP/PKA signaling are of particular interest. Between two major subtypes of PKA, type II PKA is often localized to subcellular compartments for coupling to specific downstream targets through a large family of AKAPs (a kinase-anchoring proteins; Tasken and Aandahl, 2004; for review see Wong and Scott, 2004). Such spatial targeting of PKA to specific cellular locations and signaling partners through the interaction of PKA regulatory subunits with AKAPs (Hausken et al., 1994; Hausken and Scott, 1996) has been demonstrated to be crucial for many cellular functions (Carnegie and Scott, 2003; Tasken and Aandahl, 2004; for review see Wong and Scott, 2004), including PKA regulation of muscle contractibility (Ruehr et al., 2004) and synaptic plasticity (Bauman et al., 2004). Whether the spatial targeting of PKA is important for guidance signaling in growth cones is not clear. A recent study of axon guidance in *Drosophila melanogaster* suggests that the plexin A–binding protein Nervy functions as an AKAP to antagonize semaphorin 1A–plexin A-mediated repulsion by linking cAMP/PKA to plexin A receptor (Terman and Kolodkin, 2004). In the present study, we used cultured embryonic *Xenopus laevis* neurons to dissect the cAMP signaling mechanisms. We first investigated the subcellular distribution of the two major PKA subtypes in *Xenopus* growth cones and found that type II, not type I, PKA was highly enriched in filopodia. Disruption of the filopodial localization of type II PKA abolished cAMP effects on growth cone guidance. Next, we identified a PP1 regulatory protein, inhibitor-1 (I-1), as the target of PKA in cAMP regulation of growth cone turning responses to several guidance molecules. Furthermore, we observed a colocalization of type II PKA, I-1, and PP1 in growth cone filopodia, indicating that the spatial coupling of these signaling components is important for cAMP regulation of growth cone responses. Finally, we found that I-1 and PP1 mediated growth cone repulsion induced by MAG. These findings indicate that distinct subcellular localization of type II PKA represents an important mechanism for specific cAMP/PKA signaling in growth cone guidance.

## Results

### Localization of type II PKA to growth cone filopodia

To examine the spatial distribution of two major PKA subtypes, type I and II, in *Xenopus* neurons, antibodies against their regulatory subunits (RI and RII) were used for immunofluorescent labeling. The reactivity and specificity of these antibodies to *Xenopus* tissues were confirmed by Western blotting (Fig. 1 A). Double immunofluorescence shows that both subtypes of PKA were present in *Xenopus* spinal neurons but with remarkably different spatial patterns (Fig. 1, B–D). Type I PKA was distributed evenly throughout the soma, the axonal shaft, and the central region of the growth cone (Fig. 1 B). In contrast, type II PKA was highly enriched in the peripheral region of the growth cone and, strikingly, in filopodia (Fig. 1 B). A close examination of the growth cones at a higher resolution shows that RII was predominantly concentrated in filopodia where RI was least abundant (Fig. 1, C and D). The distinct spatial patterns of PKA subtypes are clearly evidenced in color images merged from two channels (Fig. 1, B–D; red, RII; green, RI). If the RII antibody was premixed with saturating recombinant human RIIβ in otherwise the same immunostaining, the RII immunofluorescence in filopodia disappeared. However, RI staining was largely unaffected (Fig. 1 E), further confirming the specificity of the RII antibody in our immunostaining.

To quantitatively demonstrate the filopodial enrichment of PKA RII, we measured the immunofluorescence intensity of RI and RII in three regions of the neuron: the filopodia, the growth cone (excluding filopodia), and the adjacent axonal shaft (see the schematic diagram in Fig. 1 H). The measurements from the filopodia and the growth cone were normalized against that from the axonal shaft (Fig. 1 H). The results show that the filopodial RII immunofluorescence was approximately threefold stronger than that of the axonal shaft, whereas the RI immunofluorescence was the lowest in filopodia (Fig. 1 H). Similar spatial patterns of RII and RI were also observed in cultured rat hippocampal neurons (Fig. S1, available at http://www.jcb.org/cgi/content/full/jcb.200607128/DC1; and see Fig. 4 A). Together, our findings indicate a spatial enrichment of type II PKA in growth cone filopodia that could play an important role in growth cone guidance.

The type II PKA is often targeted to subcellular domains by AKAPs (Tasken and Aandahl, 2004; for review see Wong and Scott, 2004). Using a previously described PKA RII overlay approach (Williams, 2002), we found several bands from *Xenopus* neural tube tissues that were eliminated by Ht31 but not Ht31P peptides (Fig. S2, available at http://www.jcb.org/cgi/content/full/jcb.200607128/DC1). Ht31 encodes the PKA RII–binding sequence of a human thyroid AKAP (Carr et al., 1992) and is widely used for the competitive and specific disruption of PKA RII–AKAP binding, whereas Ht31P is the negative control derived from Ht31 with two amino acids mutated (Colledge and Scott, 1999). This result suggests the presence of AKAPs in *Xenopus* neurons. To directly test the role of AKAPs in PKA localization in *Xenopus* growth cones, we treated the neuronal culture with a membrane-permeable Ht31 peptide (stearated Ht31 [St-Ht31]) and found that the filopodial localization of RII was greatly reduced (Fig. 1 F), whereas the control peptide St-Ht31P was ineffective (Fig. 1 G). Quantitative analysis shows that St-Ht31, not St-Ht31P, largely reduced RII enrichment in the filopodia (Fig. 1 H). Importantly, the RI distribution remained unaffected under both St-Ht31

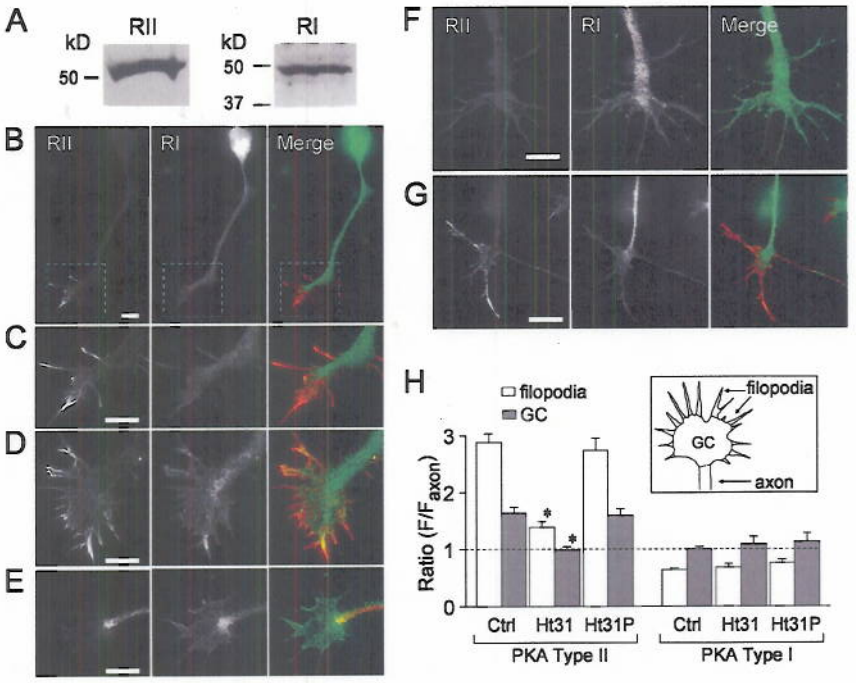


Figure 1. **Spatial distribution of type I and II PKA in cultured *Xenopus* neurons.** (A) *Xenopus* PKA regulatory subunits were detected by Western blotting with antibodies against RIIβ and RI. (B–D) Representative fluorescent images of *Xenopus* neurons stained with the aforementioned antibodies. A typical *Xenopus* neuron is shown in B, and its growth cone (indicated by the dashed boxes) is shown in an enlarged view in C. The color images are merged fluorescence of RII (red) and RI (green). (E) Representative fluorescent images of a growth cone double labeled in the presence of saturated recombinant RIIβ during primary antibody incubation. (F and G) RII and RI immunofluorescence of *Xenopus* neurons treated with 50 μM St-Ht31 for 30 min (F) or 50 μM St-Ht31P (G). (H) For quantitative analyses, the neuronal axons were arbitrarily divided into three regions (see inset): the filopodia, the growth cone (GC; excluding filopodia), and the axon (adjacent axonal shaft). For each neuron, the average fluorescence intensities of the filopodia and the growth cone were normalized against that of the axon ($F/F_{axon}$). Data from three groups of neurons are summarized and presented as the mean ± SEM (error bars). Ctrl, $n = 46$; Ht31, $n = 15$; Ht31P, $n = 12$. An asterisk indicates significant difference from the control group ($P < 0.01$; *t* test). Bars, 10 μm.

and St-Ht31P treatments (Fig. 1, F–H). It should be noted that Ht31 does not affect antibody binding to RII because Western blotting of endogenous RII was not affected by St-Ht31 (unpublished data). Therefore, these results support the notion that type II PKA is enriched in growth cone filopodia through AKAPs.

### PKA localization by AKAPs is required for cAMP regulation of growth cone guidance

Because filopodia are involved in directional responses of growth cones to guidance cues (Chien et al., 1993; Kater and Rehder, 1995; Zheng et al., 1996; Gomez et al., 2001), the localization of type II PKA in filopodia suggests a potential role in growth cone guidance. To test this notion, growth cone turning assays were performed in which a guidance gradient was established by pulsatile pressure ejection of a guidance solution from a micropipette (Lohof et al., 1992; Zheng et al., 1994a). Relatively large and motile growth cones of cultured *Xenopus* spinal neurons on laminin were used for assessing turning responses to several extracellular gradients (Guirland et al., 2003; Wen et al., 2004). We first examined growth cone attraction induced by a gradient of membrane-permeant cAMP analogues (Lohof et al., 1992; Guirland et al., 2003). A Sp-cAMPS gradient (20 mM in the ejection pipette and ~20 μM reaching the growth cone) induced a marked attraction of *Xenopus* growth cones within 30 min (Fig. 2 A). When 2 μM St-Ht31 was added to the bath, the attractive response to the cAMP gradient was abolished (Fig. 2 B), whereas 2 μM Ht31P had no effect (Fig. 2 C). We quantified the turning response of each growth cone by measuring its turning angle and net length of extension. A majority of the growth cones turned toward the Sp-cAMPS pipette (attraction) to bear a positive turning angle, which is depicted by the cumulative distribution of the turning angles (Fig. 2 D, top). In the presence of St-Ht31, growth cones did not exhibit any directional preference during the 30-min exposure to the Sp-cAMPS gradient (Fig. 2 D, top). The effective blockade of cAMP-induced attraction by St-Ht31 is also highlighted by the average turning angle from all of the growth cones examined (Fig. 2 E). For all of these manipulations, the growth cone extension remained similar (Fig. 2 E), indicating that only the directional response of growth cones was affected.

We also examined growth cone attraction induced by a gradient of pituitary adenylate cyclase–activating polypeptide (PACAP), a neuropeptide that is known to activate G protein–coupled receptors to elevate cytosolic cAMP levels (Vaudry et al., 2000). As we reported previously (Guirland et al., 2003), a PACAP gradient (1 μM in the pipette and ~1 nM at the growth cone) induced a marked attraction of *Xenopus* growth cones (Fig. 2 D, bottom). However, the attraction was completely attenuated by the bath application of St-Ht31 but not by St-Ht31P (Fig. 2, D [bottom] and E). Similarly, the net growth cone extension under these manipulations did not show any significant difference ($P > 0.05$; Fig. 2 E). To verify that the blockade of cAMP-induced turning was not a result of the nonspecific effect of Ht31, we examined growth cone attraction induced by a gradient of neurotrophin-3 (NT-3), which has been shown to be independent of cAMP signaling (Song et al., 1998; Song and Poo, 1999). We found that St-Ht31 treatment had no influence on NT-3–induced attraction (Fig. 2 E). Collectively, our data indicate that growth cone attraction induced by local cAMP signaling depends on the spatial localization of type II PKA via AKAPs.

One profound effect of the cAMP pathway on $Ca^{2+}$-dependent growth cone guidance is to switch repulsion to

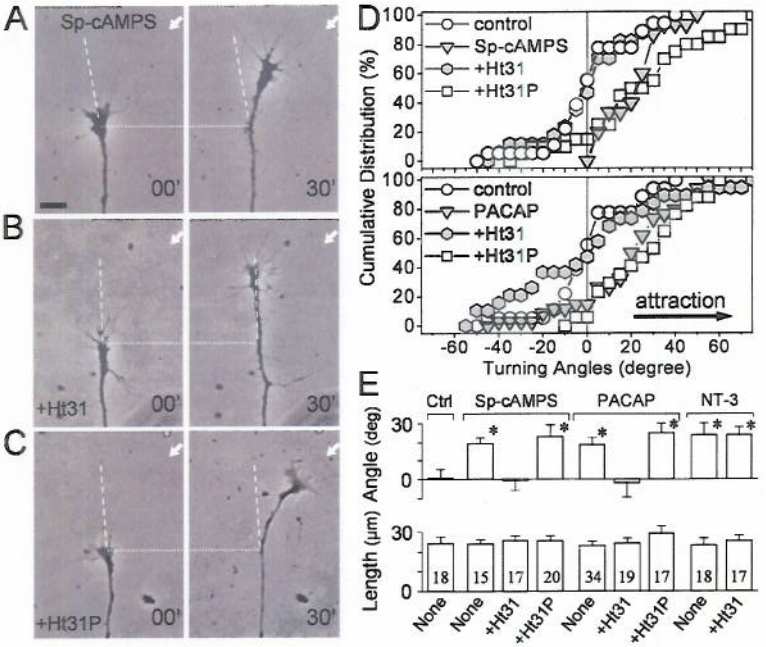


Figure 2. **Growth cone attraction induced by local PKA activation depends on type II PKA anchoring.** (A–C) Representative images showing the *Xenopus* growth cones at the onset and end of a 30-min exposure to a Sp-cAMPS gradient (20 mM in pipette) without (A) and with the bath application of 2 μM St-Ht31 (B) or 2 μM St-Ht31P (C). Dashed lines represent the original directions of growth cone extension, and dotted lines indicate the starting positions of the growth cone. Arrows indicate the directions of the gradients. Bar, 10 μm. (D) Cumulative distributions of turning angles summarize the effects of St-Ht31 and St-Ht31P on the growth cone responses to Sp-cAMPS (top; 20 mM in pipette) and PACAP (1 μM in the pipette). The control was obtained when normal bath solution was in the pipette. Each point depicts the percentage of growth cones bearing a turning angle equal to or less than the value indicated on the x axis. Positive angles indicate attraction. (E) Average turning angles and lengths of net growth cone extension for each condition are shown. The turning responses induced by NT-3 (50 μg/ml in the pipette) serve as the control. Error bars represent SEM. An asterisk indicates significant difference from the control group ($P < 0.01$; Mann-Whitney test). Numbers indicate the total growth cones examined for each group.

attraction through PKA activation or vice versa (Song and Poo, 1999). We examined the role of type II PKA and its spatial localization in the switching of turning responses. *Xenopus* growth cones plated on the laminin surface exhibited an attractive response to a gradient of brain-derived neurotrophic factor (BDNF; 50 μg/ml in the pipette and ~50 ng/ml at the growth cone), which could be converted to repulsion by PKA inhibition through the bath application of 20 μM Rp-cAMPS (Fig. 3; Song et al., 1997; Guirland et al., 2004). We found that the bath application of 2 μM St-Ht31 led to growth cone repulsion in response to the same BDNF gradient, whereas St-Ht31P had no effect (Fig. 3). Considering that BDNF-induced attraction was similarly converted to repulsion by either PKA inhibition (Rp-cAMPS) or the blockade of PKA–AKAP interaction (Ht31), it is likely that type II PKA and its localized activity in filopodia are required to support the attractive growth cone response to BDNF.

We next examined growth cone repulsion in response to a gradient of MAG, a key inhibitory molecule in axon regeneration after injury in the central nervous system (Filbin, 2003). In our *Xenopus* cultures, a gradient of MAG effectively induced the repulsive turning of most growth cones to result in a negative average turning angle (Fig. 3). PKA activation by Sp-cAMPS was able to convert MAG repulsion to attraction, resulting in a positive average turning angle (Fig. 3; Song et al., 1998). Bath application of either 2 μM St-Ht31 or St-Ht31P alone did not affect the repulsion induced by MAG gradients. However, St-Ht31 was able to abolish the switching of MAG repulsion to attraction by Sp-cAMPS (Fig. 3). Consistently, growth cone extension was not significantly affected by these treatments ($P > 0.05$; Fig. 3). Finally, we found that NT-3–induced attraction was not affected by Ht31 treatment but was switched to repulsion by Rp-cGMPS (Fig. 3). These results are consistent with previous findings that the guidance effects of BDNF and MAG involve $Ca^{2+}$ signals and can be modulated by the cAMP pathway, whereas NT-3 is independent of $Ca^{2+}$ and can only be modulated by the cGMP pathway (Song and Poo, 1999). Our findings further indicate that the spatial localization of type II PKA (and its activity) in growth cone filopodia through AKAPs is required for $Ca^{2+}$-dependent attractive responses.

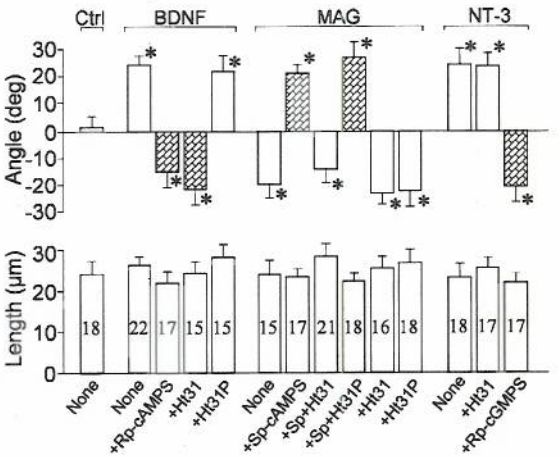


Figure 3. **Type II PKA anchoring is required for the switching of turning responses by cAMP.** Average turning angles and lengths of net growth cone extension show the turning responses of *Xenopus* growth cones to BDNF (50 μg/ml in pipette), MAG (100 μg/ml in pipette), and NT-3 (50 μg/ml in pipette) gradients with and without bath exposure to cAMP analogues and antagonists. To disrupt RII–AKAP interactions, 2 μM St-Ht31 or St-Ht31P was added in the bath 30 min before the onset of turning assays. Patterned bars indicate switching of the turning response from its original one. Error bars represent SEM. An asterisk indicates significant difference from the control group ($P < 0.01$; Mann-Whitney test). Numbers indicate the total growth cones examined for each group.

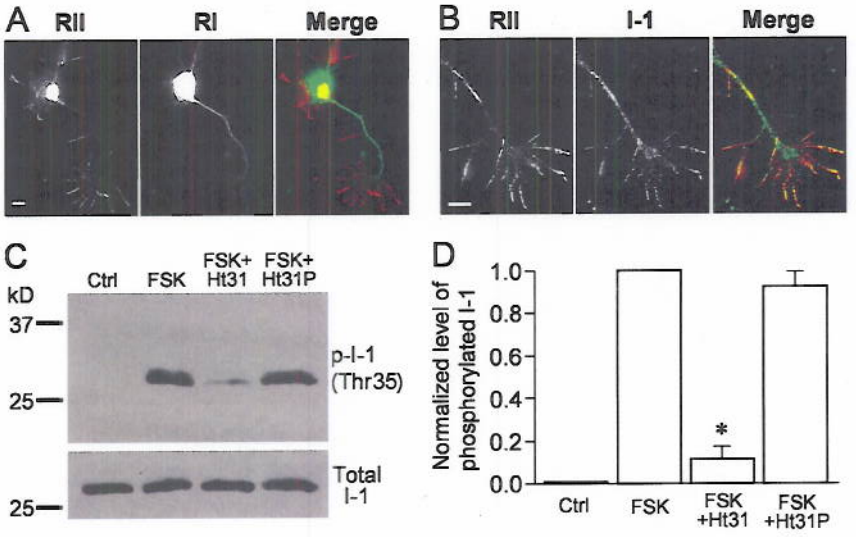


Figure 4. **PKA phosphorylation of I-1 requires type II PKA anchoring via AKAPs.** (A) Immunofluorescent images of a typical rat hippocampal neuron labeled by antibodies recognizing RII and RI. The color panel is the merged fluorescence of the two channels (RII, red; RI, green). (B) Double staining of RII and I-1 in another hippocampal neuron growth cone, with the color panel showing the merged fluorescence (RII, red; I-1, green). (A and B) Bars, 5 μm. (C and D) The effects of 20 μM St-Ht31 and St-Ht31P on forskolin (FSK)-induced I-1 phosphorylation at Thr35 in hippocampal neurons as revealed by Western blotting (C). The phosphorylation level of each condition is normalized by total I-1. Quantification of the data from three independent experiments is shown in D. Error bars represent SEM. The asterisk indicates significant difference compared with the forskolin-treated group ($P < 0.01$; *t* test).

### I-1 is the downstream target of type II PKA signaling in growth cone turning

Localization of PKA via AKAPs is thought to couple PKA activity to specific downstream targets, a mechanism that is believed to control cAMP spatiotemporal signaling in the cell (Tasken and Aandahl, 2004; for review see Wong and Scott, 2004). Our previous study suggests that PKA regulates $Ca^{2+}$-dependent growth cone turning through the inhibition of PP1 (Wen et al., 2004). PP1 activity is known to be regulated by a regulatory protein, I-1, whose phosphorylation by PKA at Thr35 leads to PP1 inhibition, and dephosphorylation by calcineurin (CaN) relieves the inhibition (Ceulemans and Bollen, 2004). Because PP1 inhibition appears to be important for cAMP switching of $Ca^{2+}$-dependent repulsion to attraction (Wen et al., 2004), we tested whether I-1 is a key substrate for spatially localized type II PKA in guidance regulation. Because our *Xenopus* cultures typically contain a large population of myocytes, we used rat hippocampal cultures for biochemical analysis of I-1 phosphorylation and its dependence on AKAPs. At first, we performed immunofluorescent staining and found that PKA RII was also enriched in the growth cone filopodia of cultured hippocampal neurons (2–3 d in vitro; Fig. 4 A), which is consistent with our observations on *Xenopus* neurons. Using an antibody recognizing I-1, we found that I-1 was also enriched in filopodia and colocalized with PKA RII (Fig. 4 B). Western blot analysis using a phosphospecific I-1 antibody showed that the level of phosphorylated I-1 was very low at rest but was markedly increased upon forskolin treatment for cAMP elevation (20 μM for 20 min). The PKA phosphorylation of I-1 was largely abolished when the cells were incubated with St-Ht31 but not St-Ht31P for 30 min before forskolin stimulation (Fig. 4 C). Quantification of the data from three independent blotting analyses shows that the phosphorylation of I-1 by forskolin treatment was reduced by ~90% upon Ht31 disruption of the RII–AKAP interaction (Fig. 4 D). These results indicate that spatially anchored type II PKA accounts for a large part of I-1 phosphorylation in neurons, particularly in the growth cone filopodia.

We next examined the distribution of I-1 in *Xenopus* growth cones and its role in guidance. Similar to hippocampal neurons, I-1 was found to be concentrated in filopodia and colocalized with PKA RII (Fig. 5 A). To understand the function of I-1 in growth cone guidance, we used I-1 morpholino (IM) antisense oligonucleotides to knock down the I-1 level in *Xenopus* neurons through the microinjection of one-cell–stage *Xenopus* embryos. As the control, a morpholino oligonucleotide of scrambled sequence (control morpholino [CM]) was used. We found that IM effectively knocked down the expression level of I-1 in injected *Xenopus* embryos around stage 20, as indicated by Western blotting using the whole embryo lysates (Fig. 5 B). In contrast, CM injection did not affect the endogenous I-1 level. Importantly, IM did not change the expression levels of PKA RII and PP1γ (Fig. 5 B), demonstrating the specificity of I-1 knockdown by the morpholino approach. To test the functional role of I-1 in growth cone guidance, *Xenopus* spinal neuron cultures were prepared from both IM- and CM-injected embryos, and cultured neurons exhibiting the fluorescence of coinjected Oregon green–dextran (Fig. 5 C) were selected for turning assay. Immunostaining of I-1 in IM-injected cells did not detect a substantial level of I-1, supporting the Western blot result that I-1 was greatly reduced by IM (Fig. 5 C). When we exposed these I-1 knockdown growth cones to a gradient of Sp-cAMPS or PACAP, no preferential turning was induced (Fig. 5 D). On the other hand, growth cones of CM-injected neurons responded positively to the cAMP and PACAP gradients (Fig. 5 D). Again, the average lengths of growth cone extension were not significantly different among various groups ($P > 0.05$; Fig. 5 E). Therefore, these results provide evidence that I-1 is a key molecule that mediates cAMP-induced growth cone attraction. Given that I-1 and RII are colocalized in filopodia, spatial targeting of PKA to I-1 in filopodia may be a crucial step in cAMP/PKA signaling that regulates growth cone turning.

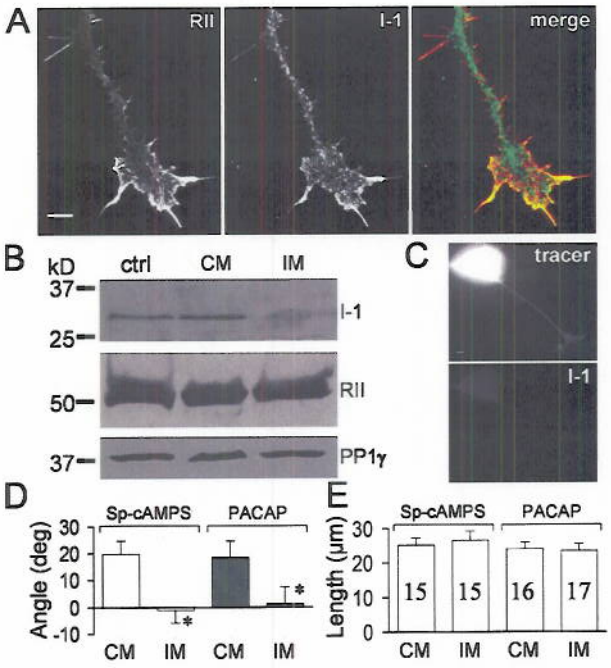


Figure 5. **I-1 mediates PKA-induced growth cone attraction.** (A) I-1 distribution in a *Xenopus* spinal neuron and its colocalization with RII. The color panel represents the merged channels of RII (red) and I-1 (green). (B) A specific I-1 morpholino (IM) or control morpholino (CM) was injected into *Xenopus* embryos, and the efficiency and specificity of knockdown were examined by Western blotting of whole embryo lysates at stages 20–22 using antibodies against I-1 (top), RII (middle), and PP1γ (bottom). The results are representative of at least three independent experiments. (C) Morpholino oligonucleotides were coinjected with a fixable Oregon green–dextran that could be traced in spinal neuron cultures. *Xenopus* neurons that are tracer positive (i.e., IM injected; top) exhibit weak I-1 staining (bottom). (A and C) Bars, 5 μm. (D and E) Average turning angles and lengths of net neurite extension showing the turning responses of *Xenopus* growth cones of IM- or CM-injected neurons to cAMP and PACAP gradients. Error bars represent SEM. An asterisk indicates significant difference from CM neurons ($P < 0.01$; Mann-Whitney test). Numbers indicate the total growth cones examined for each group.

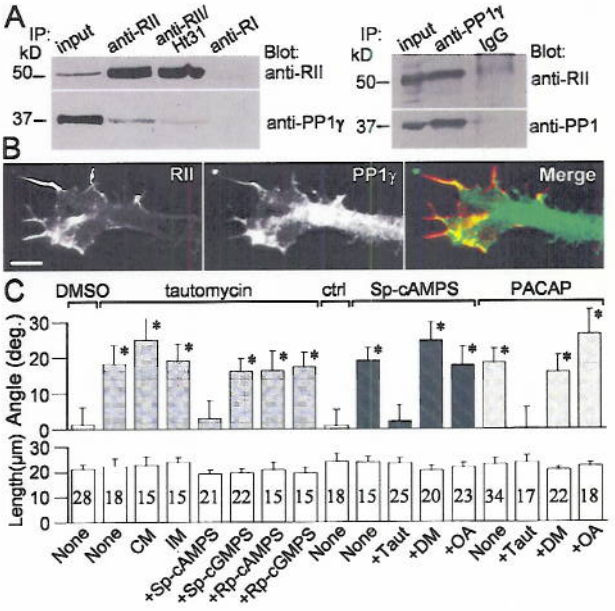


Figure 6. **PP1 mediates PKA-induced growth cone attraction.** (A) *Xenopus* neural tube tissues were immunoprecipitated with RII antibody (with or without 20 μM St-Ht31), RI antibody (left), or PP1γ antibody (right). The presence of RII and PP1γ in the precipitates was detected by Western blotting. IPs with normal IgGs were used as negative controls. The bands in the input lane indicate the normal locations of the two proteins. (B) Double staining of RII and PP1γ in a typical *Xenopus* neuron. The merged color image shows the colocalization of RII (red) and PP1γ (green) in the filopodia. Bar, 5 μm. (C) Turning responses induced by either cAMP and PACAP gradients or local PP1 inhibition. The chemicals shown at the top of the graph were loaded into ejection pipettes at the following concentrations: 10% DMSO, 3 μM tautomycin, 20 mM Sp-cAMPS, and 1 μM PACAP. The turning assays were performed in normal bath solution or in solutions containing the following individual reagents: 20 μM of cyclic nucleotide analogues, 3 nM tautomycin (Taut), 1 nM of the PP2A inhibitor okadaic acid (OA), or 10 nM of the CaN inhibitor deltamethrin (DM). Error bars represent SEM. An asterisk indicates significant difference from the control group ($P < 0.01$; Mann-Whitney test). Numbers indicate the total growth cones examined for each group.

### PP1 inhibition is a key event downstream of PKA activation for guidance regulation

Many AKAPs not only bind PKA holoenzymes but also recruit other molecules to create signaling complexes, which is believed to be important for signal integration as well as for the efficiency and specificity of PKA activity (Tasken and Aandahl, 2004; for review see Wong and Scott, 2004). We hypothesized that PKA inhibition of PP1 through I-1 may also involve a similar mechanism to regulate growth cone responses to guidance molecules. We first performed coimmunoprecipitation (co-IP) using *Xenopus* neural tube tissues to examine whether type II PKA and PP1 were present in a signaling complex. Using specific antibodies against PKA RII and PP1γ, we found that a small amount of PP1γ could be consistently pulled down by RII (but not by RI) and vice versa (Fig. 6 A). Importantly, the PP1γ signal decreased when co-IP was performed in the presence of St-Ht31 (Fig. 6 A). In support of the co-IP data, double immunofluorescence labeling also revealed the substantial colocalization of PP1γ with PKA RII in *Xenopus* growth cone filopodia, although PP1γ fluorescence was also distributed in the axon (Fig. 6 B). Together with the aforementioned results, these observations suggest that spatially restricted formation of the signaling complex involving PKA, I-1, and PP1 in filopodia constitutes an important mechanism for the efficient and specific cAMP signaling that regulates growth cone turning.

To further test the model that PKA exerts its regulation on growth cone turning primarily through the inhibition of PP1, we used the turning assay to examine the effects of the direct inhibition of PP1 using specific inhibitors. We first tested the notion that growth cone attraction induced by a gradient of cAMP involves a local (asymmetric) inhibition of PP1. Here, a gradient of the PP1 inhibitor tautomycin was generated by pulsatile ejection of 3 μM tautomycin solution from the pipette (estimated ~3 nM at the growth cone). We found that asymmetric inhibition of PP1 by the tautomycin gradient elicited a marked attractive turning of *Xenopus* growth cones (Fig. 6 C). As a crucial control, we also examined the attractive response to the tautomycin gradient in neurons containing morpholino oligonucleotides and found that neither IM nor CM affected the attraction

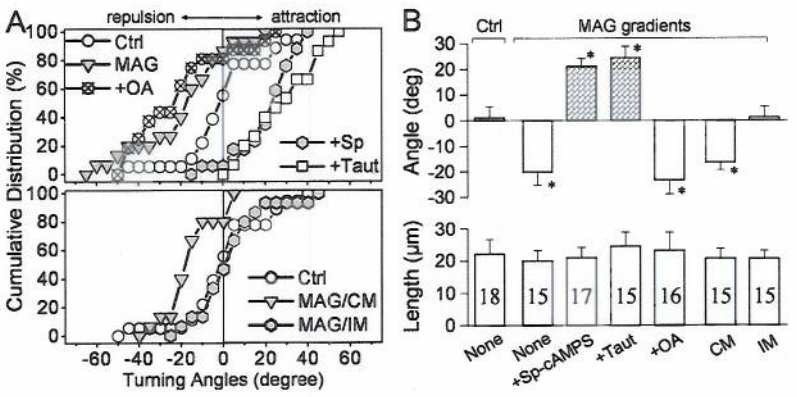


Figure 7. **I-1 and PP1 mediate MAG-induced growth cone repulsion.** (A) The cumulative distributions of turning angles depict the growth cone responses to a gradient of MAG-Fc (100 μg/ml in the pipette) with and without PP1 inhibition (top) and I-1 knockdown (bottom). 20 μM Sp-cAMPS, 3 nM tautomycin (Taut,), and 1 nM OA were all added to the bath 30 min before the onset of turning assays. (B) Average turning angles and net growth cone extension for each condition are depicted. Patterned bars indicate switching of the turning response from its original one. Error bars represent SEM. An asterisk indicates significant difference from the control group ($P < 0.01$; Mann-Whitney test). Numbers indicate the total growth cones examined for each group.

(Fig. 6 C). Such results are expected because tautomycin directly inhibits PP1 without the involvement of I-1. To confirm that local PKA activation and PP1 inhibition are in the same signaling pathway to induce growth cone turning, we performed a series of cross-desensitization experiments. In the first set, we examined tautomycin-induced attraction in the presence of various cyclic nucleotides in bath. Tautomycin was found to lose its ability to attract growth cones only after Sp-cAMPS application (Fig. 6 C), supporting the notion that cAMP/PKA targets PP1 activity. In the second set of experiments, growth cone attraction induced by Sp-cAMPS or PACAP gradients was performed with or without tautomycin in bath. We found that the global inhibition of PP1 by tautomycin abolished the turning responses induced by both Sp-cAMPS and PACAP gradients (Fig. 6 C). In contrast, 1 nM of the PP2A inhibitor okadaic acid (OA) and 10 nM of the CaN inhibitor deltamethrin did not affect these turning responses (Fig. 6 C). Collectively, these findings support the idea that the asymmetric inhibition of PP1 at the growth cone by cAMP gradients mediates the attractive turning responses.

### I-1 and PP1 mediate MAG-induced growth cone repulsion

MAG is a key inhibitory molecule in axon regeneration in the central nervous system (Filbin, 2003). MAG-induced growth cone repulsion has been shown to involve $Ca^{2+}$ and can be switched to attraction by cAMP (Song et al., 1998; Henley et al., 2004). In our *Xenopus* cultures, a gradient of MAG consistently induced growth cone repulsion, and the repulsion could be converted to attraction by the bath application of Sp-cAMPS (Fig. 7 A, top). Importantly, MAG-induced growth cone repulsion was also effectively converted to attraction by PP1 inhibition through the bath application of 3 nM tautomycin. The low concentration of tautomycin we used (3 nM) is known to mainly inhibit PP1, although higher concentrations of tautomycin could inhibit another protein phosphatase, PP2A ($IC_{50}$ = 10 nM). To confirm that the conversion of MAG repulsion to attraction by tautomycin specifically involved PP1 inhibition, we examined MAG-induced repulsion when PP2A was inhibited by 1 nM OA. Our data show that OA did not affect MAG-induced repulsion (Fig. 7 A, top). The average turning angles and lengths of growth cone extension in these groups are summarized in the bar graphs for comparison (Fig. 7 B). It is clear that either PKA activation by Sp-cAMPS or PP1 inhibition by tautomycin converted the MAG-induced repulsion to attraction in a similar way, suggesting that PP1 is a target of the cAMP regulation of MAG repulsion. Interestingly, when the endogenous I-1 in *Xenopus* neurons was greatly reduced by IM, MAG-induced repulsion was completely abolished, whereas CM did not affect MAG-induced repulsion (Fig. 7). The complete blockade of MAG-induced repulsion together with data on the involvement of PP1 indicates that I-1 and PP1 are involved in signal transduction in MAG repulsion.

## Discussion

The major cAMP pathway is believed to involve the activation of PKA, which, in turn, phosphorylates a variety of downstream substrates for distinct signaling cascades. It is interesting to note that cAMP molecules can diffuse over long distances in the cytosol (Kasai and Petersen, 1994), and PKA does not possess a high degree of substrate selectivity (Shabb, 2001). Thus, the target specificity and phosphorylation efficiency of PKA in a distinct signaling pathway are believed to involve spatial coupling of PKA to its appropriate downstream effectors through a large family of AKAPs (Tasken and Aandahl, 2004; for review see Wong and Scott, 2004). It has been shown that type II PKA is the major subtype that associates with AKAPs and often exhibits localized subcellular distribution (Tasken and Aandahl, 2004; for review see Wong and Scott, 2004). In the present study, we present evidence that spatially distributed type II PKA is involved in growth cone guidance. The striking localization of type II PKA in growth cone filopodia indicates that it may be involved in regulation of the actin cytoskeleton dynamics underlying growth cone motility and guidance. Using the turning assay, we have provided direct evidence that the spatial localization of type II PKA in filopodia is required for cAMP-induced growth cone turning and switching of turning responses to guidance gradients. Furthermore, we have obtained evidence that PKA acts on PP1 through I-1 (all localized in filopodia) to regulate growth cone turning responses. These findings indicate an exciting model in which spatial targeting of PKA to its downstream targets in growth cone filopodia allows the profound cAMP regulation of growth cone responses to guidance cues.

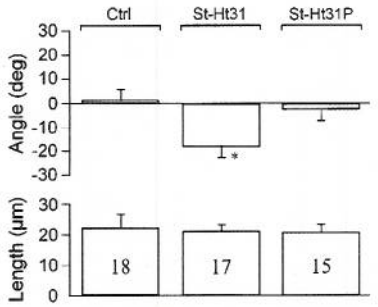


Figure 8. **Growth cone turning induced by local disruption of the AKAP–RII interaction.** In the presence of Sp-cAMPS (20 μM in bath), a gradient of St-Ht31 (2 mM in the pipette and ~2 μM reaching the growth cone) induced repulsive turning. The St-Ht31P gradient (2 mM in the pipette) is a control and had no effect. Average turning angles and lengths of net growth cone extension for each condition are depicted. Error bars represent SEM. An asterisk indicates significant difference from the control group ($P < 0.01$; Mann-Whitney test). Numbers indicate the total growth cones examined for each group.

There is a large body of studies demonstrating that AKAPs are the major family of scaffolding proteins for the subcellular localization of PKA molecules (for review see Wong and Scott, 2004). The predominant localization of type II PKA in growth cone filopodia is likely mediated by AKAPs because it was diminished by the inhibitory peptide St-Ht31 (Fig. 1). Moreover, the peptide abolished cAMP-induced growth cone turning and switching of guidance responses (Figs. 2 and 3). These results evince that AKAP-mediated PKA localization in filopodia is crucial for local cAMP signaling during growth cone guidance. In support of this notion, we found that a gradient of St-Ht31 induced repulsive turning in the presence of bath Sp-cAMPS (Fig. 8), indicating that local cAMP signaling can be achieved by the spatial regulation of PKA–AKAP interaction. It should be noted that a much higher concentration of St-Ht31 was used to diminish the localization of PKA RII in filopodia than that used to block turning responses. This is likely caused by the fact that Ht31 competes for PKA RII binding and that a higher concentration is required to remove PKA RII molecules that have already bound to AKAPs at the filopodia. On the other hand, cAMP regulation of growth cone turning may require dynamic PKA–AKAP interactions, which could be affected by low concentrations of the Ht31 peptides. This intriguing notion will be tested in future studies.

Another interesting observation came from the immunostaining experiment in which anti-RII antibodies were premixed with recombinant RII proteins (Fig. 1 E). Although filopodial staining was eliminated, strong signals in the axonal shaft were detected, which is a reversal of the results from standard immunostaining using only the anti-RII antibody (Fig. 1, B–D). Because unoccupied AKAPs in fixed cells could bind RII in situ (Hausken et al., 1998), this observation suggests the availability of unoccupied RII-binding sites (potentially of AKAPs) in the axonal shaft but not in filopodia. At this moment, the mechanisms underlying this fascinating local enrichment of PKA RII in filopodia but not in other regions of the neuron remain unknown. It is plausible that the AKAPs in filopodia may have a much higher affinity for binding RII and/or that the affinity is spatially regulated (Ruehr et al., 2004; for review see Wong and Scott, 2004). Alternatively, the expression level of PKA RII may be limited so that PKA RII is mostly recruited (or translocated) to filopodia. Currently, the exact AKAPs involved in PKA localization in growth cone filopodia are not known. Our RII overlay assay revealed several bands that might represent potential AKAPs (Fig. S2). Filopodia are actin-based motile membrane protrusions that are known to play an important role in growth cone motility and sensing of extracellular signals. The preferential enrichment of type II PKA in filopodia indicates that PKA may be associated with the actin cytoskeleton to regulate filopodial dynamics in a spatially restricted manner. A similar role of spatially anchored type II PKA has been implicated in chemotactic cells (Howe et al., 2005). Moreover, our co-IP experiments suggest that type II PKA and PP1 interact (either directly or indirectly) in *Xenopus* neurons. Thus, AKAPs that exhibit actin- and PP1-binding properties are, in principle, the good candidates (for review see Wong and Scott, 2004). Future identification of the AKAPs involved in filopodia localization of PKA RII will substantially advance the understanding of the mechanisms and functions of PKA spatial localization in growth cone guidance.

The second major finding of this study is that the PKA inhibition of PP1 through I-1 acts as a key mechanism underlying cAMP regulation of growth cone guidance. Our previous work has shown that local activation of the CaN–PP1 pathway by $Ca^{2+}$ signals induces repulsion, and cAMP activation of PKA inhibits the CaN–PP1 repulsive pathway to allow the conversion of repulsion to attraction (Wen et al., 2004). In this study, we provided evidence that I-1 is a target of PKA and CaN that oppositely controls PP1 activity for distinct turning responses (Fig. 9). Specifically, I-1 knockdown by morpholino abolished growth cone turning in response to local cAMP elevation (Fig. 5). However, I-1 knockdown did not affect growth cone turning induced by the direct local inhibition of PP1 by tautomycin (Fig. 6), confirming that I-1 acts upstream of PP1 in regulating growth cone turning. Dopamine- and cAMP-regulated phosphoprotein of 32 kD (DARPP-32) and I-1 are the two best-characterized PKA-activated inhibitors of PP1. I-1 is widely expressed in mammalian tissues, whereas DARPP-32 is mainly found in dopaminoceptive brain regions with very low expression levels in the spinal cord and hippocampus (Hemmings and Greengard, 1986). DARPP-32 is not expressed in the *Xenopus* oocyte (Maton et al., 2005), but it is not clear whether it is expressed in *Xenopus* embryos around the developmental stages we studied. Although the antibody we used can recognize both proteins (~30 kD), we believe that I-1 is the one that is expressed in *Xenopus* neurons and is involved in growth cone guidance. This notion is supported by the observation that specific *Xenopus* I-1 morpholino antisense almost completely eliminated the signals by Western blotting and immunofluorescence using the I-1/DARPP-32 antibody.

MAG is an important component of inhibitory molecules in central nervous system axon regeneration, and one important insight into MAG signaling came from the observation that MAG-induced repulsion was blocked by I-1 knockdown. A previous study indicates that MAG-induced repulsive turning

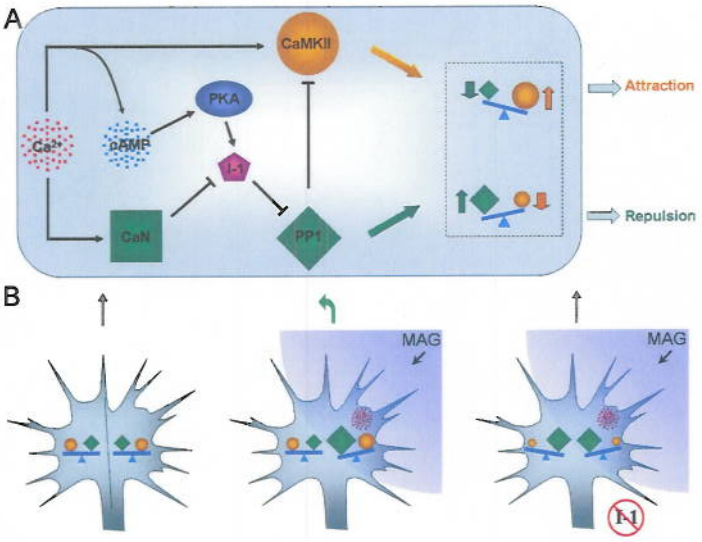


Figure 9. **Schematic diagrams illustrate the model on how $Ca^{2+}$ and cAMP control the turning responses of growth cones.** (A) A modified model involving the CaMKII/CaN–PP1 switch (Wen et al., 2004) and the role of PKA and I-1 in growth cone turning. According to this model, a local imbalance of CaMKII and PP1 activity is the key for generating distinct turning responses. A higher CaMKII or lower PP1 activity favors attraction, whereas a lower CaMKII or higher PP1 activity leads to repulsion. (B) Based on our data, MAG-induced repulsion involves $Ca^{2+}$ signals (red) that locally elevate PP1 activity, resulting in an imbalance of PP1/CaMKII activity for repulsion. In I-1 knockdown neurons, the MAG gradient can no longer regulate PP1 activity asymmetrically to induce repulsion. Furthermore, PP1 activity is likely elevated as a result of the loss of I-1, which can inhibit CaMKII to prevent attractive turning.

involves small local $Ca^{2+}$ elevations (Henley et al., 2004), which likely act through CaN–PP1 (Wen et al., 2004). Because CaN dephosphorylates I-1 at Thr35 (Thr34 for *Xenopus*) to remove its inhibition on PP1, the local $Ca^{2+}$ activation of CaN would lead to the local elevation of PP1 activity for repulsive turning. The fact that the direct inhibition of PP1 was able to convert the MAG effect to attraction provides direct support for $Ca^{2+}$-CaN–PP1 in MAG signaling during repulsion. Morpholino knockdown of I-1 disrupts the signaling transduction from CaN to PP1, thus resulting in the blockade of repulsion. However, unlike PP1 inhibition or PKA activation, I-1 knockdown did not convert MAG-induced repulsion to attraction but instead abolished turning responses. Previous studies have indicated that a spatial balance of Ca-calmodulin–dependent kinase II (CaMKII) and PP1 activities control the bidirectional steering of the growth cones (Fig. 9 A; Wen et al., 2004; Gomez and Zheng, 2006). Importantly, $Ca^{2+}$-dependent attraction involves the local activation of CaMKII, which can be dephosphorylated and inhibited by PP1 (Blitzer et al., 1998; Colbran, 2004). Therefore, the loss of I-1 by morpholino knockdown could result in elevated PP1 activity (Carr et al., 2002) to prevent the local CaMKII activation required for attraction (Fig. 9 B).

Increasing evidence indicates that the spatiotemporal control of cascades of signaling reactions in confined subcellular locations is key for intricate signal transduction occurring in the living cells. This study has established that spatial targeting of PKA to filopodia allows the signal transduction through cAMP, type II PKA, I-1, and PP1 to regulate growth cone turning. Given the apparent localization of PKA RII, I-1, and some PP1 in filopodia, it is conceivable that interactions between type II PKA and PP1 may affect the activity of molecules that regulate the actin cytoskeleton and/or membrane-substrate adhesion. For instance, PP1 is found to directly dephosphorylate actin-depolymerizing factor/cofilin (Meberg et al., 1998), thereby promoting actin depolymerization. It is also possible that PP1 may modulate $Ca^{2+}$ signals through the negative regulation of $Ca^{2+}$ channels and stores (Ceulemans and Bollen, 2004) to influence $Ca^{2+}$-dependent guidance. Our study has also provided additional support for the model that a spatial balance of CaMKII and CaN–PP1 activity controls bidirectional steering of the growth cone (Fig. 9 A). In principle, growth cone attraction can be induced by either the local elevation of CaMKII (e.g., by moderate $Ca^{2+}$ signals) or by the local inhibition of PP1 (e.g., by local cAMP/PKA activation or direct inhibition of PP1). In the latter case, baseline CaMKII activity would be required to generate a higher CaMKII/PP1 ratio on the near side of the growth cone for attraction. Indeed, global inhibition of CaMKII by KN93 abolished the attraction induced by tautomycin and cAMP gradients (unpublished data). In parallel, repulsion can be induced by either the local elevation of PP1 activity (e.g., by $Ca^{2+}$-CaN activation) or by the local inhibition of CaMKII. Together, our findings indicate a model in which the spatial regulation of signal localization and activity balance controls the directional motility of growth cones in response to extracellular stimuli (Fig. 9 A).

## Materials and methods

### Antibodies and reagents

Antibodies against different antigens used in this study are as follows: PKA RIIβ (BD Biosciences); PKA RII and RI, PP1, and PP1γ (Santa Cruz Biotechnology, Inc.); I-1/DARPP-32 (Chemicon); and phospho–I-1/DARPP-32 (Novus Biologicals). Recombinant rat MAG-Fc was purchased from R&D Systems, and recombinant human BDNF was provided by Regeneron. PACAP was obtained from American Peptide. PKA RII proteins were provided by the laboratory of S. Taylor (University of California, San Diego, La Jolla, CA) as well as purchased from Biaffin GmbH and Co KG. St-Ht31 and St-Ht31P were purchased from Promega. Cyclic nucleotides (Sp-cAMPS, Rp-cAMPS, Sp-cGMPS, and Rp-cGMPS), tautomycin, deltamethrin, OA, and forskolin were all obtained from Calbiochem. A morpholino antisense oligonucleotide specific for I-1 was designed and synthesized by Gene Tools, LLC, with the sequence 5′-ATGGAGGCGAACAGTCCCAGGAAGA-3′. A control morpholino was used with the sequence 5′-CCTCTTACCTCAGTTACAATTTATA-3′.

### Cell cultures and embryo microinjection

Embryonic cultures of *Xenopus* spinal neurons were prepared from neural tube tissues of stage 20–22 embryos and plated on coverslips coated with poly-D-lysine and laminin (Sigma-Aldrich) in a serum-free medium as

described previously (Guirland et al., 2003). The serum-free medium consisted of 50% (vol/vol) Leibovitz L-15 medium (Sigma-Aldrich), 50% (vol/vol) Ringer's solution (115 mM NaCl, 2 mM $CaCl_2$, 2.5 mM KCl, and 10 mM Hepes, pH 7.6), and 1% (wt/vol) BSA (Sigma-Aldrich). *Xenopus* cultures were maintained at 20–22°C for 6–10 h before fixation or were used for the turning assay. In I-1 knockdown experiments, I-1 or control morpholino oligonucleotides together with a fixable Oregon green–dextran conjugate (Invitrogen) were injected into the animal pole of one-cell *Xenopus* embryos (Alder et al., 1995). The injected embryos were screened 24 h later for the presence of fluorescence and were used for cell culture. For turning assays, the cells exhibiting the green fluorescence of Oregon green–dextran were used.

Primary hippocampal neurons were prepared from embryonic day 18 rat embryos (Banker and Cowan, 1977), plated on coverslips or into culture dishes coated with poly-D-lysine at a density of ~600,000 cells/ml (for Western blotting) or ~100,000 cells/ml (for immunofluorescence), and incubated at 37°C with 5% $CO_2$ in MEM supplemented with 10% FBS (Invitrogen), 0.5% glucose, 1 mM sodium pyruvate, 25 μM glutamine, and 1× penicillin-streptomycin. The next day after plating, the medium was changed to the Neurobasal medium (Invitrogen) supplemented with 1× B27 supplement (Invitrogen). For immunofluorescence experiments, neurons were fixed after 2–3 d in vitro. For Western blotting, neurons were first treated with different drugs on day in vitro 5 and then were lysed in radioimmunoprecipitation buffer (50 mM Tris, 50 mM NaF, 2 mM EDTA, 150 mM NaCl, 1% Triton X-100, 0.25% sodium deoxycholate, 0.4 mM $Na_3VO_4$, 1 mM PMSF, 1 mg/ml leupeptin, 5 mg/ml chymostatin, 1 mg/ml pepstatin, and 5 mM E64). All studies involving vertebrate animals (frogs and rats) are performed in accordance with the National Institutes of Health (NIH) guidelines and were approved by the Institutional Animal Care and Use Committee of the University of Medicine and Dentistry of New Jersey.

### Immunofluorescence and quantification of fluorescence intensity

Cells on coverslips were fixed with 4% PFA in a cacodylate buffer (Guirland et al., 2003) for 30 min at room temperature and were permeabilized with 0.5% Triton X-100 for 10 min. Samples were blocked overnight in 10% BSA in PBS followed by sequential incubation with primary and secondary antibodies. Coverslips were mounted on slides and visualized through a 60× NA 1.4 plan Fluor oil immersion objective (Nikon) on an inverted epifluorescence microscope (TE2000; Nikon) equipped with a CCD camera (SensiCam QE; Cooke Scientific). Fluorescence images were taken using IPLab software (version 3.7; BD Biosciences) and transferred to ImageJ software (NIH) for fluorescence intensity measurement and color coding and merging. The settings for imaging and processing were fixed throughout the experiments. Quantification of the fluorescence intensity was performed by first subtracting the background and then measuring the average intensity from the regions of interest that were hand traced using ImageJ. For the axonal shaft, we simply placed an oval region in the shaft for measurement of the intensity. Measurements from each growth cone were normalized, and results from multiple growth cones were then averaged.

### Immunoprecipitation and Western blotting

*Xenopus* neural tube tissues were lysed in the radioimmunoprecipitation buffer, and the clarified lysates were incubated with antibodies against RII (with or without St-Ht31), RI, PP1-γ, or normal IgG (Santa Cruz Biotechnology, Inc.) overnight at 4°C. Immune complexes were isolated by incubation with protein A/G PLUS agarose (Santa Cruz Biotechnology, Inc.) for 2 h at 4°C. Cell lysates or IP samples were separated on NuPAGE Novex 3–8% Tris-acetate gels (Invitrogen) or 10% Tris-glycine gels and were transferred to nitrocellulose membranes. After incubation with appropriate primary antibodies, the membranes were detected by HRP-conjugated secondary antibodies and ECL reagents (GE Healthcare).

### Growth cone turning induced by extracellular chemical gradients

Growth cone turning induced by chemical gradients was performed with a modified Ringer's solution (115 mM NaCl, 2.6 mM KCl, 1 mM $MgCl_2$, 1 mM $CaCl_2$, and 10 mM Hepes, pH 7.6) as described previously (Ming et al., 1999; Guirland et al., 2004). Microscopic gradients of chemicals were produced by repetitive pressure ejection through a micropipette with an opening of 1 μm (pressure of 3 pounds per square inch, repetition of 2 Hz, and duration of 20 ms). Under these settings, the concentration of the chemical reaching the growth cone is estimated to be ~1/1,000th of that in the pipette (Lohof et al., 1992; Zheng et al., 1994a). The original direction of growth cone extension at the beginning of the experiment was defined by the distal 20-μm segment of the neurite. The pipette tip was positioned 45° from the initial direction of extension and 100 μm away from the growth cone. Different reagents were added to the bath medium 20 min before the onset of turning assays. To quantify the turning responses, digital images of the growth cone at the onset and end of the 30-min turning assay were acquired and overlaid with pixel-to-pixel accuracy, and the trajectory of new neurite extension was traced using Photoshop (Adobe). The turning angle was defined by the angle between the original direction of neurite extension and a line connecting the positions of the growth cone at the onset and end of the experiment. A positive angle resulted from turning toward the pipette and vice versa. Neurite extension was quantified by measuring the trajectory of net neurite extension over the 30-min period. Only growth cones that extended 5 μm or more were scored and analyzed for turning responses. We used the nonparametric Mann-Whitney test to analyze turning angles (expressed as mean ± SEM) because they do not follow a normal distribution.

### Online supplemental material

Fig. S1 shows the filopodia localization of PKA RII in cultured hippocampal neurons. Fig. S2 shows the existence of potential AKAPs in *Xenopus* neural tube tissues through an RII overlay assay. Online supplemental material is available at http://www.jcb.org/cgi/content/full/jcb.200607128/DC1.

We would like to thank Dr. Renping Zhou (Rutgers University, Piscataway, NJ) for his help on this project and Dr. Susan Taylor for providing recombinant PKA RII proteins.

This research is supported by grants from NIH (NS036241) and the New Jersey Commission on Spinal Cord Research (NJCSCR; 04-3029-SCR) to J.Q. Zheng as well as a postdoctoral fellowship from NJCSCR to J. Han (grant 06-2918-SCR).

Submitted: 24 July 2006
Accepted: 1 December 2006

## References

Alder, J., H. Kanki, F. Valtorta, P. Greengard, and M.M. Poo. 1995. Overexpression of synaptophysin enhances neurotransmitter secretion at *Xenopus* neuromuscular synapses. *J. Neurosci.* 15:511–519.

Aubert, I., J.L. Ridet, and F.H. Gage. 1995. Regeneration in the adult mammalian CNS: guided by development. *Curr. Opin. Neurobiol.* 5:625–635.

Bahr, M., and F. Bonhoeffer. 1994. Perspectives on axonal regeneration in the mammalian CNS. *Trends Neurosci.* 17:473–479.

Banker, G.A., and W.M. Cowan. 1977. Rat hippocampal neurons in dispersed cell culture. *Brain Res.* 126:397–425.

Bauman, A.L., A.S. Goehring, and J.D. Scott. 2004. Orchestration of synaptic plasticity through AKAP signaling complexes. *Neuropharmacology.* 46:299–310.

Blitzer, R.D., J.H. Connor, G.P. Brown, T. Wong, S. Shenolikar, R. Iyengar, and E.M. Landau. 1998. Gating of CaMKII by cAMP-regulated protein phosphatase activity during LTP. *Science.* 280:1940–1942.

Carnegie, G.K., and J.D. Scott. 2003. A-kinase anchoring proteins and neuronal signaling mechanisms. *Genes Dev.* 17:1557–1568.

Carr, A.N., A.G. Schmidt, Y. Suzuki, F. del Monte, Y. Sato, C. Lanner, K. Breeden, S.L. Jing, P.B. Allen, P. Greengard, et al. 2002. Type 1 phosphatase, a negative regulator of cardiac function. *Mol. Cell. Biol.* 22:4124–4135.

Carr, D.W., Z.E. Hausken, I.D. Fraser, R.E. Stofko-Hahn, and J.D. Scott. 1992. Association of the type II cAMP-dependent protein kinase with a human thyroid RII-anchoring protein. Cloning and characterization of the RII-binding domain. *J. Biol. Chem.* 267:13376–13382.

Ceulemans, H., and M. Bollen. 2004. Functional diversity of protein phosphatase-1, a cellular economizer and reset button. *Physiol. Rev.* 84:1–39.

Charron, F., and M. Tessier-Lavigne. 2005. Novel brain wiring functions for classical morphogens: a role as graded positional cues in axon guidance. *Development.* 132:2251–2262.

Chien, C.B., D.E. Rosenthal, W.A. Harris, and C.E. Holt. 1993. Navigational errors made by growth cones without filopodia in the embryonic *Xenopus* brain. *Neuron.* 11:237–251.

Colbran, R.J. 2004. Protein phosphatases and calcium/calmodulin-dependent protein kinase II-dependent synaptic plasticity. *J. Neurosci.* 24:8404–8409.

Colledge, M., and J.D. Scott. 1999. AKAPs: from structure to function. *Trends Cell Biol.* 9:216–221.

Dickson, B.J. 2002. Molecular mechanisms of axon guidance. *Science.* 298:1959–1964.

Filbin, M.T. 2003. Myelin-associated inhibitors of axonal regeneration in the adult mammalian CNS. *Nat. Rev. Neurosci.* 4:703–713.

Gomez, T.M., and J.Q. Zheng. 2006. The molecular basis for calcium-dependent axon pathfinding. *Nat. Rev. Neurosci.* 7:115–125.

Gomez, T.M., E. Robles, M. Poo, and N.C. Spitzer. 2001. Filopodial calcium transients promote substrate-dependent growth cone turning. *Science.* 291:1983–1987.

Guirland, C., K.B. Buck, J.A. Gibney, E. DiCicco-Bloom, and J.Q. Zheng. 2003. Direct cAMP signaling through G-protein-coupled receptors mediates growth cone attraction induced by pituitary adenylate cyclase- activating polypeptide. *J. Neurosci.* 23:2274–2283.

Guirland, C., S. Suzuki, M. Kojima, B. Lu, and J.Q. Zheng. 2004. Lipid rafts mediate chemotropic guidance of nerve growth cones. *Neuron.* 42:51–62.

Harel, N.Y., and S.M. Strittmatter. 2006. Can regenerating axons recapitulate developmental guidance during recovery from spinal cord injury? *Nat. Rev. Neurosci.* 7:603–616.

Hausken, Z.E., and J.D. Scott. 1996. Properties of A-kinase anchoring proteins. *Biochem. Soc. Trans.* 24:986–991.

Hausken, Z.E., V.M. Coghlan, C.A. Hastings, E.M. Reimann, and J.D. Scott. 1994. Type II regulatory subunit (RII) of the cAMP-dependent protein kinase interaction with A-kinase anchor proteins requires isoleucines 3 and 5. *J. Biol. Chem.* 269:24245–24251.

Hausken, Z.E., V.M. Coghlan, and J.D. Scott. 1998. Overlay, ligand blotting, and band-shift techniques to study kinase anchoring. *Methods Mol. Biol.* 88:47–64.

Hemmings, H.C., Jr., and P. Greengard. 1986. DARPP-32, a dopamine- and adenosine 3′:5′-monophosphate-regulated phosphoprotein: regional, tissue, and phylogenetic distribution. *J. Neurosci.* 6:1469–1481.

Henley, J.R., K.H. Huang, D. Wang, and M.M. Poo. 2004. Calcium mediates bidirectional growth cone turning induced by myelin-associated glycoprotein. *Neuron.* 44:909–916.

Howe, A.K., L.C. Baldor, and B.P. Hogan. 2005. Spatial regulation of the cAMP-dependent protein kinase during chemotactic cell migration. *Proc. Natl. Acad. Sci. USA.* 102:14320–14325.

Kasai, H., and O.H. Petersen. 1994. Spatial dynamics of second messengers: IP3 and cAMP as long-range and associative messengers. *Trends Neurosci.* 17:95–101.

Kater, S.B., and V. Rehder. 1995. The sensory-motor role of growth cone filopodia. *Curr. Opin. Neurobiol.* 5:68–74.

Lohof, A.M., M. Quillan, Y. Dan, and M.M. Poo. 1992. Asymmetric modulation of cytosolic cAMP activity induces growth cone turning. *J. Neurosci.* 12:1253–1261.

Maton, G., T. Lorca, J.A. Girault, R. Ozon, and C. Jessus. 2005. Differential regulation of Cdc2 and Aurora-A in *Xenopus* oocytes: a crucial role of phosphatase 2A. *J. Cell Sci.* 118:2485–2494.

Meberg, P.J., S. Ono, L.S. Minamide, M. Takahashi, and J.R. Bamburg. 1998. Actin depolymerizing factor and cofilin phosphorylation dynamics: response to signals that regulate neurite extension. *Cell Motil. Cytoskeleton.* 39:172–190.

Ming, G., H. Song, B. Berninger, N. Inagaki, M. Tessier-Lavigne, and M. Poo. 1999. Phospholipase C-gamma and phosphoinositide 3-kinase mediate cytoplasmic signaling in nerve growth cone guidance. *Neuron.* 23:139–148.

Nishiyama, M., A. Hoshino, L. Tsai, J.R. Henley, Y. Goshima, M. Tessier-Lavigne, M.M. Poo, and K. Hong. 2003. Cyclic AMP/GMP-dependent modulation of Ca2+ channels sets the polarity of nerve growth-cone turning. *Nature.* 423:990–995.

Ooashi, N., A. Futatsugi, F. Yoshihara, K. Mikoshiba, and H. Kamiguchi. 2005. Cell adhesion molecules regulate Ca2+-mediated steering of growth cones via cyclic AMP and ryanodine receptor type 3. *J. Cell Biol.* 170:1159–1167.

Qiu, J., D. Cai, H. Dai, M. McAtee, P.N. Hoffman, B.S. Bregman, and M.T. Filbin. 2002. Spinal axon regeneration induced by elevation of cyclic AMP. *Neuron.* 34:895–903.

Richter-Landsberg, C., and B. Jastorff. 1986. The role of cAMP in nerve growth factor-promoted neurite outgrowth in PC12 cells. *J. Cell Biol.* 102:821–829.

Ruehr, M.L., M.A. Russell, and M. Bond. 2004. A-kinase anchoring protein targeting of protein kinase A in the heart. *J. Mol. Cell. Cardiol.* 37:653–665.

Rydel, R.E., and L.A. Greene. 1988. cAmp analogs promote survival and neurite outgrowth in cultures of rat sympathetic and sensory neurons independently of nerve growth factor. *Proc. Natl. Acad. Sci. USA.* 85:1257–1261.

Shabb, J.B. 2001. Physiological substrates of cAMP-dependent protein kinase. *Chem. Rev.* 101:2381–2411.

Skaper, S.D. 2005. Neuronal growth-promoting and inhibitory cues in neuroprotection and neuroregeneration. *Ann. NY Acad. Sci.* 1053:376–385.

Song, H.J., and M.M. Poo. 1999. Signal transduction underlying growth cone guidance by diffusible factors. *Curr. Opin. Neurobiol.* 9:355–363.

Song, H.J., G.L. Ming, and M.M. Poo. 1997. cAMP-induced switching in turning direction of nerve growth cones. *Nature.* 388:275–279.

Song, H., G. Ming, Z. He, M. Lehmann, L. McKerracher, M. Tessier-Lavigne, and M. Poo. 1998. Conversion of neuronal growth cone responses from repulsion to attraction by cyclic nucleotides. *Science.* 281:1515–1518.

Spencer, T., and M.T. Filbin. 2004. A role for cAMP in regeneration of the adult mammalian CNS. *J. Anat.* 204:49–55.

Tasken, K., and E.M. Aandahl. 2004. Localized effects of cAMP mediated by distinct routes of protein kinase A. *Physiol. Rev.* 84:137–167.

Terman, J.R., and A.L. Kolodkin. 2004. Nervy links protein kinase a to plexin-mediated semaphorin repulsion. *Science.* 303:1204–1207.

Tessier-Lavigne, M., and C.S. Goodman. 1996. The molecular biology of axon guidance. *Science.* 274:1123–1133.

Vaudry, D., B.J. Gonzalez, M. Basille, L. Yon, A. Fournier, and H. Vaudry. 2000. Pituitary adenylate cyclase-activating polypeptide and its receptors: from structure to functions. *Pharmacol. Rev.* 52:269–324.

Wen, Z., C. Guirland, G.L. Ming, and J.Q. Zheng. 2004. A CaMKII/calcineurin switch controls the direction of Ca(2+)-dependent growth cone guidance. *Neuron.* 43:835–846.

Williams, R.O. 2002. Cutting edge: A-kinase anchor proteins are involved in maintaining resting T cells in an inactive state. *J. Immunol.* 168:5392–5396.

Wong, W., and J.D. Scott. 2004. AKAP signalling complexes: focal points in space and time. *Nat. Rev. Mol. Cell Biol.* 5:959–970.

Zheng, J.Q., M. Felder, J.A. Connor, and M.M. Poo. 1994a. Turning of nerve growth cones induced by neurotransmitters. *Nature.* 368:140–144.

Zheng, J.Q., Z. Zheng, and M. Poo. 1994b. Long-range signaling in growing neurons after local elevation of cyclic AMP-dependent activity. *J. Cell Biol.* 127:1693–1701.

Zheng, J.Q., J.J. Wan, and M.M. Poo. 1996. Essential role of filopodia in chemotropic turning of nerve growth cone induced by a glutamate gradient. *J. Neurosci.* 16:1140–1149.